行政院國家科學委員會補助專題研究計畫成果報告

※※※※※※※※※※※※※※※※※※※※※※※※※※

※　高透射率嵌附層、唯相移層、極短紫外光反射式圖罩吸收層　※

※　與緩衝層之材料、電漿蝕刻與性質探討　※

※　※

※※※※※※※※※※※※※※※※※※※※※※※※※※

計畫類別：☑個別型計畫　　□整合型計畫

計畫編號：NSC92－2215－E－009－066

執行期間：　92 年　8 月　1 日至 93 年　7 月　31 日

計畫主持人：龍文安

共同主持人：

計畫參與人員：葉文隆，林志鴻，林政旻

執行單位：交通大學應用化學系

中　華　民　國　　93 年　10　月 25 日

高透射率嵌附層、唯相移層、極短紫外光反射式圖罩吸收層與緩衝層之材料、電漿蝕刻與性質探討

Studies on materials, plasma etchings and properties of high T% embedded layers, shifter only layers, extreme uv reflective mask's absorbers and buffers

計畫編號：NSC92-2215-E-009-066

執行期間：92 年 8 月 1 日 至 93 年 7 月 31 日

主持人：龍文安　交通大學應用化學系教授

一、中文摘要

申請三年計畫，因僅核定第一年計畫，故僅執行第一年計畫。本計畫探討193奈米微影嵌附式減光型相移圖罩之高透射率(>30%)嵌附層, 其材料、光學、物性、化性、電漿蝕刻等性質，並應用於嵌附式減光型相移圖罩。

英文摘要

Studies on optical, physical, chemical and plasma etching properties of high transmittance embedded layer (T>30 %) and its application on the embedded attenuated PSM (EAPSM).

1. Introduction

According to the Semiconductor Industry Association (SIA) lithography roadmap, 0.13 and 0.1 μm technology generation is expected to be achieved in 2002 and 2005, respectively.[1] An argon fluoride (ArF) exposure line, combined with attenuated phase-shifting mask (AttPSM) and off-axis illumination, would enable optical lithography for the manufacture of LSI devices below the 0.13 μm design rule. However, the higher transmittance of the embedded layer in AttPSM with clear tone provides better contrast of aerial images and a process window for contact holes.[2] Therefore, ArF with the high-transmittance AttPSM might extend optical lithography to the 0.1 or even 0.07 μm design rule.

The optical properties of the embedded layer govern whether it can be applied to enhance the resolution of patterns. However, in order to provide efficient productivity, embedded materials also must have good chemical stability, including cleaning, exposure and environment durability. Although many embedded materials for the AttPSM blank in 193 nm lithography have been developed,[3–5] the method of achieving the chemical stability of the embedded layer has not been well studied. We report a novel method of achieving the chemical stability of embedded materials. The correlation between chemical compositions and sputtering conditions is studied to achieve the chemical stability of the embedded layer. The bi layer $AlSi_xO_y$ embedded layer presents good chemical stability, including cleaning and environment durability. Using a Helicon wave etcher and Taguchi methodology for the design of the experiment, a 0.2 μm etched pattern for AttPSM in 193 nm lithography using $AlSi_xO_y$ as an embedded layer is successfully fabricated.

This paper also reported the application of a simulation of high-transmittance ($T\% > 15\%$) AttPSM with dark tone for 0.1 μm contact hole patterns. The resolution of the contact pattern increased with increasing transmittance of AttPSM. However, if the transmittance of AttPSM is too large, a side-lobe pattern will be generated. Here, a special design of the mask, in which the side lobe for high-transmittance AttPSM is avoided, will be studied.

2. Experiment

$AlSi_xO_y$ films were formed into be bi layer embedded material on fused silica substrates. Bi layer $AlSi_xO_y$ films were formed by plasma sputtering of Al (90–210 W) and Si (40–100 W) under Ar (86 sccm) and O_2 (0.5–3.5 sccm) using an Ion Tech Merovac 450 C sputtering system. Transmittance $T\%$ and reflectance $R\%$ were determined using a Shimadzu UV-2501PC double-beam UV-VIS spectrometer. The R-T method[6] was used to determine n and k of $AlSi_xO_y$ films. The thicknesses of $AlSi_xO_y$ films and substrate fused silica SiO_2 were measured using a Dektak 3030 surface profilometer and a Hitachi S-400 field emission-scanning electron microscope (FE-SEM). The atomic ratio of thin films was measured with a Jeol JXA-8800M EPMA. Physical Electronics PHI 1600 ESCA with a Mg K_α standard source under a scan of 0.2 eV was used to analyze the chemical compositions of thin films. Cross sectional profiles of patterns of the resist and embedded layer were taken using a Hitachi S-400 FE-SEM.

The patterning of resist on the $AlSi_xO_y$ film was carried out using a Leica EBML-300 e-beam exposure system. An Anelva ILD-4100 helicon wave etcher was employed to study the etching selectivity and to fabricate the patterns on the $AlSi_xO_y$ embedded layer.

The application of high-transmittance AttPSM was simulated with lithography software Prolith Ver. 7.01 (Finel). The exposure conditions in 193 nm lithography were three NAs, 0.55, 0.6 and 0.65, quadrupole illumination, resist thickness of 0.3–0.4 μm and SiO_xN_y BARC thickness of 0.055 μm.

Dark- and clear-tone masks with high-transmittance AttPSM were used to study the effect of transmittance on the formation of side lobes.

3. Results and Discussion

3.1 Chemical stability of embedded material

Most embedded materials can be formed by sputtering. Usually, by controlling the sputtering conditions, suitable optical properties for 248 or 193 nm wavelength could be obtained. However, there is no clear rule for forming embedded material with good chemical stability and optical properties simultaneously. Thus, a method of achieving good chemical stability of embedded material is very important. Here, a novel method of achieving chemical stability has been studied. If the correlation among sputtering conditions, chemical compositions and optical properties of embedded material could be clarified, an embedded material with good chemical stability would be easily generated.

The embedded layer, $AlSi_xO_y$, could be ordinarily formed by a combination of SiO_2 and Al_2O_3 of transparent chemical compositions, and Si and Al of absorbing elements, as shown in Fig. 1. If the sputtering condition is controlled well, n, k, T% and R% of $AlSi_xO_y$ films are kept in the range of high transmittance ($T\% = 15$–35%), enabling $AlSi_xO_y$ to be used as an embedded material. The T% 15%, 35% and R% 15%, 20% curves are calculated by the R-T method under phase shifting of 180 degrees. The critical sputtering parameters are Al target power and O_2 flow rate. The rates of Al_2O_3 (Al, 2p, 75.6 eV) and SiO_2 (Si, 2p, 102.9 eV) formation increased while those of Al (Al, 2p, 73.1 eV) and Si (Si, 2p, 99.2 eV) formation decreased with increasing O_2 flow rate, as shown in Fig. 2. It was assumed that the silicon and aluminum atoms become linked to more oxygen atoms with increasing oxygen content. Compared to Al and Si compositions, Al_2O_3 and SiO_2 have lower k and higher n, as shown in Fig. 1. When the oxide structure increased with increasing atomic percentage of oxygen, n of $AlSi_xO_y$ appeared to increase while k appeared to decrease in 193 nm lithography, as shown in Fig. 3. The Al and Si compositions nearly disappeared at an O_2 flow rate of about 2.2 sccm, and saturation of the Al_2O_3 and SiO_2 formations was observed, as shown in Fig. 2. The correlation between Al target power and chemical compositions is also shown in Fig. 4 for Al 100–200 W, Si 70 W, Ar 86 sccm and O_2 1.6 sccm. When the Al target power increased, the optical properties of $AlSi_xO_y$ shifted to properties of film with high Al content. Therefore, n of this film decreased and k increased in 193 nm lithography, as shown in Fig. 5.

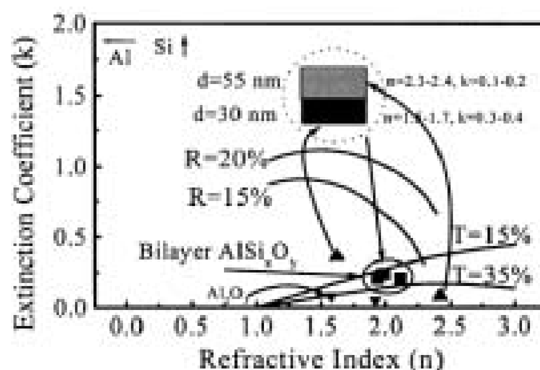

Fig. 1. The n and k plane of high-transmittance bi layer $AlSi_xO_y$ embedded layer for AttPSM in 193 nm lithography.

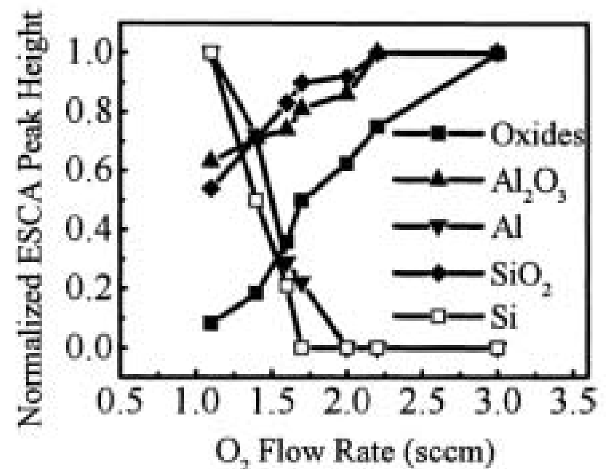

Fig. 2. Effect of oxygen flow rate on chemical composition of $AlSi_xO_y$ under conditions of Al 160 W, Si 70 W and Ar 86 sccm.

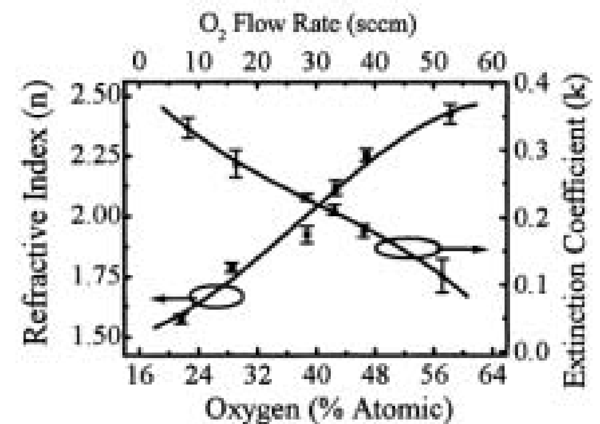

Fig. 3. Correlation between optical properties and O_2 flow rate during sputtering under conditions of Al 160 W, Si 70 W, Ar 86 sccm and O_2 0.9–3.2 sccm.

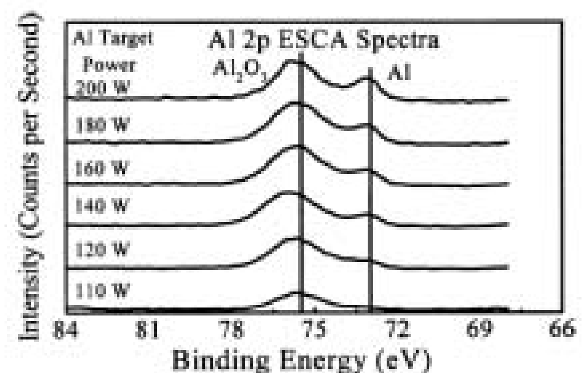

Fig. 4. Effect of Al target power on chemical composition of $AlSi_xO_y$ under conditions of Si 70 W, Ar 86 sccm and O_2 1.6 sccm.

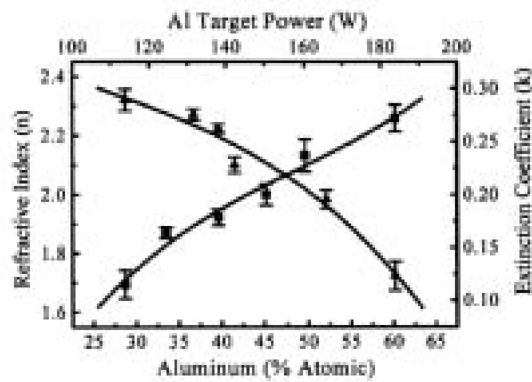

Fig. 5. Correlation between optical properties and Al target power during sputtering under conditions of Al 90–210 W, Si 70 W, Ar 86 sccm and O_2 1.6 sccm.

The correlation between chemical composition and optical properties of $AlSi_xO_y$ exhibits one clear trend. The $AlSi_xO_y$ film with saturated of Al_2O_3 and SiO_2 formation can be predicted to have good chemical stability. However, this film which has k smaller than 0.1, is too transparent to be used as $T\% \sim 15\%–35\%$ embedded material in 193 nm lithography. When the $AlSi_xO_y$ film has suitable transmittance, it contains Al and Si compositions and may not have sufficient chemical stability. Therefore, a bi layer embedded material is another option.

3.2 *Bi layer $AlSi_xO_y$ embedded material for AttPSM in 193 nm lithography*

Bi layer $AlSi_xO_y$ embedded material is a combination of a transparent layer (top layer) and an absorptive layer (bottom layer) as shown in Fig. 1. The transparent layer with saturation of Al_2O_3 and SiO_2 compositions exhibits n of 2.3–2.4 and k of 0.1–0.2. This layer was predicted to have good chemical stability and sufficient resistance to cleaning, exposure and environment. The absorptive layer with higher Al and Si exhibits n of 1.5–1.7 and k of 0.3–0.4. The Al and Si compositions were not oxidized completely. It might not have good stability, but could absorb the intensity of 193 m wavelength moderately and provide a suitable $T\% \sim 15–35\%$ bi layer $AlSi_xO_y$ film.

The cleaning durability of the transparent and absorptive layers of $AlSi_xO_y$ film are shown in Figs. 6 and 7, respectively. After SC-1 cleaning, the Si and Al peaks of the absorptive layer with higher Si and Al compositions disappeared, thus, the optical properties of $AlSi_xO_y$ changed. However, the ESCA spectra of the transparent layer were not changed. The transparent layer has good chemical stability. Although the transparent layer with saturated Al_2O_3 and SiO_2 has better chemical stability, $T\% \sim 80\%$ was too high and unsuitable for AttPSM. Therefore, two $AlSi_xO_y$ components, transparent and absorptive layers, were well combined to satisfy the demands of high transmittance and chemical stability of the embedded layer in 193 nm lithography. The top and bottom layer thicknesses are adjusted to satisfy the required $T\%$, phase angle and chemical stability of the bi layer $AlSi_xO_y$ embedded material simultaneously. The thickness of the top layer is near 55 nm and that of the bottom layer is near 30 nm.

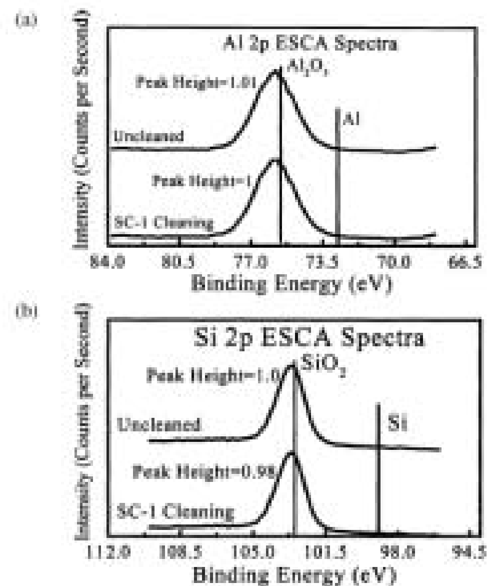

Fig. 6. ESCA spectra showing the effect of SC-1 cleaning on the chemical composition of transparent layer of bi layer $AlSi_xO_y$ films.

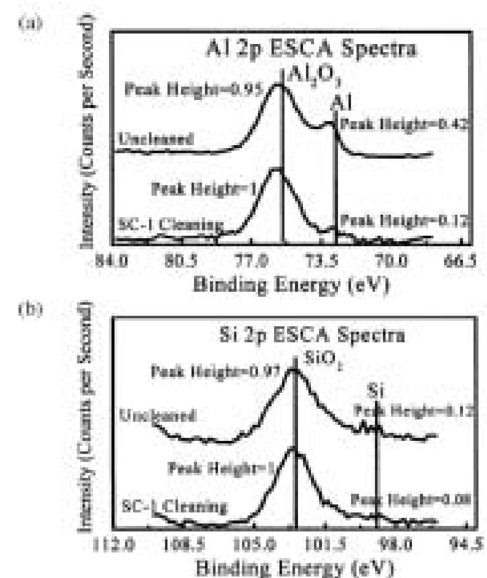

Fig. 7. ESCA spectra showing the effect of SC-1 cleaning on the chemical compositions of absorptive layer of bi layer $AlSi_xO_y$ films.

3.3 *Simulation of high-transmittance AttPSM for 0.1 μm contact pattern*

With the suitable increase of the transmittance of AttPSM, the resolution and contrast of the aerial image of a contact-hole pattern would increase. However, the risk of the generation of a side-lobe pattern is also raised. When the layout of the 0.1 μm pitch (1 : 1.5) and isolated contact pattern is designed as a clear-tone mask, the intensity of the side lobe increases with increasing transmittance of AttPSM, as shown in Fig. 8, in 193 nm lithography. I_0 is supposed as the intensity of the large blank area. I is intensity of pattern area. When the transmittance of AttPSM is 5%, the side-lobe intensity

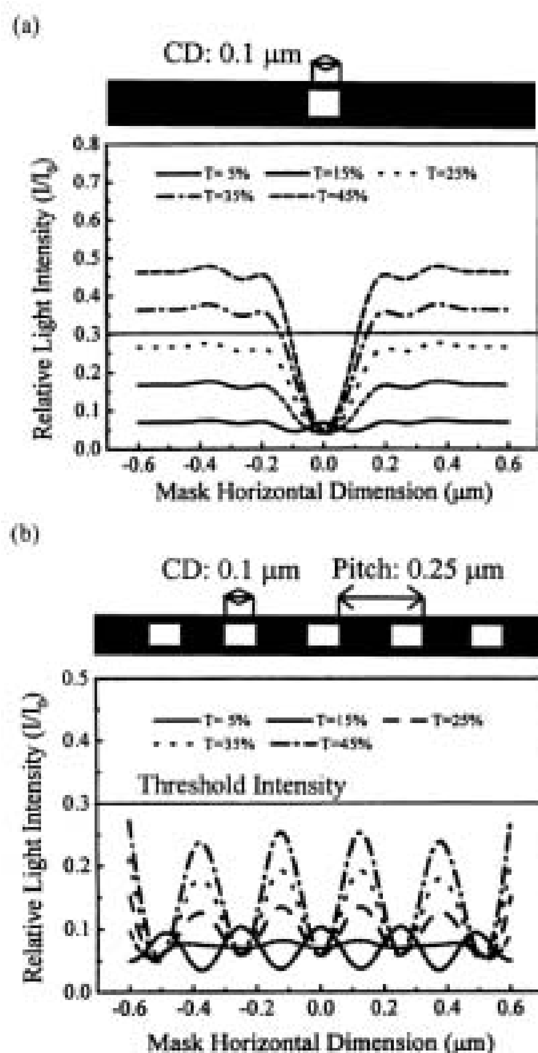

Fig. 8. The effect of transmittance of AttPSM on the resolution of aerial image of 0.1 μm (a) isolated and (b) pitch (1 : 1.5) contact holes with clear tone AttPSM in 193 nm lithography.

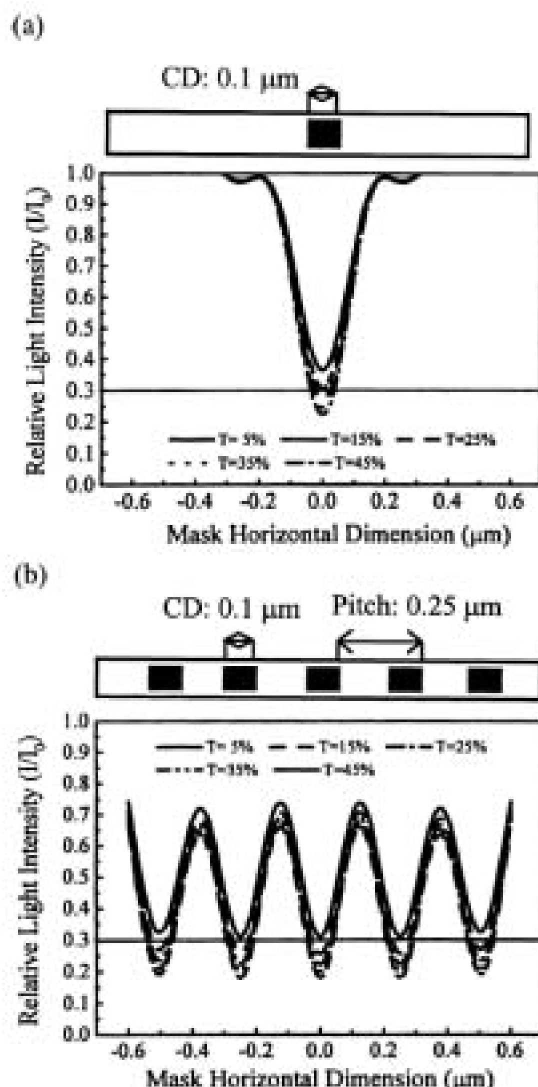

Fig. 9. The effect of transmittance of AttPSM on the resolution of aerial image of 0.1 μm (a) isolated and (b) pitch (1 : 1.5) contact holes with dark tone AttPSM in 193 nm lithography.

is very low. However, the contrast of the aerial image of the 0.1 μm contact pattern is too low at this T%. When the layout of the 0.1 μm pitch (1 : 1.5) and isolated contact pattern is designed as a dark-tone mask, the resolution of the aerial image increase with increasing T% of AttPSM, as shown in Fig. 9. Even, when the transmittance of AttPSM is 45%, the side lobe intensity is no longer generated. Because the contact pattern is small, the intensity of the electric field amplitude of the contact pattern, generated by high transmittance, could be compensated by the intensity of the clear pattern, near the edge of contact. However, if the contact pattern is designed as a dark-tone mask, a negative resist is necessary. The combination of dark-tone mask, high-transmittance AttPSM and negative resist could provide better contrast of the aerial image and resolution of the 0.1 μm contact-hole pattern in 193 nm lithography.

3.4 *Etched pattern of $AlSi_xO_y$ embedded layer*

Although the compositions of top and bottom layers of bi layer $AlSi_xO_y$ embedded layer were different, the mixed gases of O_2 + BCl_3/Cl_2 could etch this bi layer material. Only one optimized recipe could cover it under the Taguchi methodology of experiment design. However, in order to provide better etching selectivity of $AlSi_xO_y$ over chemically amplified resist NEB-22 and fused silica, two different recipes for any embedded layer would be better. In addition, the fabrication of the $AlSi_xO_y$ embedded layer should be carried out using two different etching steps. The 0.15-μm-line/space (1 : 4) NEB-22 resist profile on the $AlSi_xO_y$ embedded layer, exposed by the Leica e-beam system, had good resolution, as shown in Fig. 10(a). No footing was evident at the bottom of the resist pattern. This nearly vertical profile is transferred to the embedded layer. A 0.20-μm-line/space (1 : 1) etched pattern of the $AlSi_xO_y$ embedded layer, as illustrated in Fig. 10(b), was fabricated successfully.

(a)

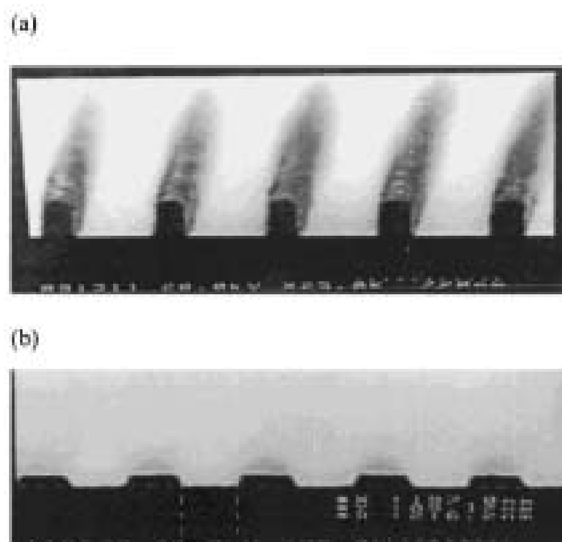

(b)

Fig. 10 (a) SEM image of a 0.15 μm line/space (1 : 3) NEB-22 resist profile on the bi layer $AlSi_xO_y$ embedded layer, (b) SEM image of a 0.20 μm line/space (1 : 1) etched pattern of bi layer $AlSi_xO_y$ embedded layer.

4. Conclusions

$AlSi_xO_y$ thin films have been developed as a new high-transmittance bi layer embedded material for AttPSM at 193 nm. The study of the correlation among sputtering conditions, chemical compositions and optical properties could lead to the chemical stability of $AlSi_xO_y$ embedded material. A 0.20-μm-line/space (1 : 1) etched pattern of the bi layer $AlSi_xO_y$ embedded material was also successfully fabricated. According to simulation experiments, the side-lobe intensity was not generated with the design of high-transmittance AttPSM and dark-tone for a 0.1 μm contact-hole pattern. Combination of the dark-tone mask, high-transmittance AttPSM and negative resist could provide better contrast of the aerial image and resolution of a 0.1 μm contact-hole pattern in 193 nm lithography.

Acknowledgements

This work was partially funded by the National Science Council and the National Chiao Tung University, Republic of China.

1) International Technology Roadmap for Semiconductors, Semiconductor Industrial Association, 1999 updated.
2) J. S. Petersen *et al.*: Proc. SPIE **3546** (1998) 188.
3) B. W. Smith, Z. Alam, S. Butt, S. Kurinec, R. L. Lane and G. Arthur: Microelectron. Eng. **35** (1997) 201.
4) U. Ushioda, Y. Seki, K. Maeda, T. Ohfuji and H. Tanabe: Jpn. J. Appl. Phys. **35** (1996) 6356.
5) Y. Seki, J. Ushioda, T. Saito, K. Maeda, K. Nakano, S. Iwasa, T. Ohfuji and H. Tanabe: Proc. SPIE **3096** (1997) 286.
6) C. M. Lin and W. A. Loong: Microelectron. Eng. **46** (1999) 93.